Oscillations of Bubbles Attached to a Capillary: Case of Pure Liquid

Vejražka, Jiří
2012

EFM12 Experimental Fluid Mechanics 2012
Hradec Králové 20th-23rd November 2012

Oscillations of bubbles attached to a capillary: case of pure liquid

J. Vejrazka[1,a], L. Vobecka[1] and J. Tihon[1]

[1]Institute of Chemical Process Fundamentals, Rozvojova 135, 165 02 Prague, Czech Republic

Abstract. An oscillating bubble attached to a tip of a capillary is used for probing interfacial properties of liquids containing surface-active agents. Nevertheless, available theories even for the case of pure liquid are not satisfactory. In this contribution, we therefore present results of a linear inviscid theory for shape oscillations of a spherical bubble, which is in contact with a solid support. The theory allows determining eigenmodes (i.e. eigenfrequencies, eigenmode shapes and damping of eigenmode oscillations), but also response of the bubble shape to a motion of its support or to volume variations. Present theory covers also the cases previously analyzed by Strani and Sabetta (J. Fluid Mech., 1984) and Bostwick and Steen (Phys. Fluids, 2009), and it can be applied to both bubbles and drops. The theory has been compared to experiments. Good agreement is found for the case of small bubbles, which have spherical static shape. Experimental results for larger bubbles and drops deviate from the theory, if a neck is formed. It is shown that this deviation correlates well with a ratio of bubble volume to the maximum volume, when a detachment occurs.

1 Introduction

Shape oscillations of drops and bubbles are extremely sensitive to the presence of surface active agents at the liquid-gas interface. For this reason, bubble/drop oscillations are of interest, if the interfacial properties like the interfacial elasticity or viscosity are studied [1,2], especially in the range of high frequencies.

Standard configuration in the equipment for measurements of the dilatational interfacial properties is a bubble or drop, which is attached to a tip of a capillary. When probing interfacial properties, volume variations are imposed to the drop in order to vary periodically its interfacial area [3]. In a different type of experiment, the supporting capillary can move, exciting shape oscillations [4].

For analyzing the shape oscillations, an assumption of irrotational flow remains reasonable, if the liquid is pure. The eigenmodes of such a supported bubble or drop are predicted by irrotational analyses of Strani and Sabetta [5] and of Bostwick and Steen [6]. These analyses differ mostly in the way how constraints due to attachment are implemented. The case studied by Bostwick and Steen was reexamined more recently with the use of more suitable approaches [7,8]. However, none of these analyses covers the cases with variable volume or moveable support, encountered in the equipment.

We have therefore developed another analytical solution [9], which is parallel to the analyses [5-8], but can deal also with variable bubble or drop volume and with the motion of bubble/drop support. In this contribution, we present result of this irrotational and linear analysis.

Experiments, in which bubble oscillations are excited by a motion of its support, have also been performed, and the observed oscillations are compared with the analytical results.

[a] vejrazka@icpf.cas.cz

2 Results of the analysis

The actual bubble shape is described by a deformation η (figure 1) from the basic spherical shape. The deformation η is a function of time t and position $\mu = \cos\theta$. For the purposes of the analysis, η is decomposed into series

$$\eta(t,\mu) = \sum_{j=0}^{N} b_j(t) P_j(\mu), \qquad (1)$$

where P_j are the Legendre polynomials. By the analysis [9], a system of differential equations for b_j coefficients is established by variational methods, and the behavior of the bubble or drop is hence entirely described. The resulting system of differential equations is

$$\mathbf{M}\frac{\mathrm{d}^2\mathbf{b}}{\mathrm{d}t^2} + 2\frac{\mu_0}{\rho_0 R^2}\mathbf{D}\frac{\mathrm{d}\mathbf{b}}{\mathrm{d}t} + \frac{\sigma}{\rho_0 R^3}\mathbf{K}\mathbf{b} = \mathbf{f}, \qquad (2)$$

where

$$\mathbf{b} = \mathbf{b}(t) = (b_1, \ldots, b_N, \lambda_1/(4\pi\sigma), \ldots, \lambda_M/(4\pi\sigma))^{\mathrm{T}} \qquad (3)$$

is the vector of N unknown coefficients b_j and of M unknown Lagrange multipliers λ_k, which are not further discussed in this text. M is the truncation order

characterizing accuracy, by which the attachment condition is satisfied ($M = 1$ or 2 is sufficient for typical attachment angles $\theta_a < 30°$). R is the radius of non-deformed bubble or drop, μ_0 and ρ_0 are the viscosity and density of the reference fluid, and σ is the interfacial tension. The mass, damping and stiffness matrices **M**, **D** and **K** are square matrices with $(N+M)^2$ elements

$$\mathbf{M}_{j,l} = \begin{cases} \dfrac{\rho_i}{\rho_0}\dfrac{1}{j(2j+1)} + \dfrac{\rho_e}{\rho_0}\dfrac{1}{(j+1)(2j+1)} & \\ \qquad \text{for } j = l = 1, 2, ..., N, & (4) \\ 0 \qquad \text{for other elements,} & \end{cases}$$

$$\mathbf{D}_{j,l} = \begin{cases} \dfrac{\mu_i}{\mu_0}\dfrac{j-1}{j} + \dfrac{\mu_e}{\mu_0}\dfrac{j+2}{j+1} & \\ \qquad \text{for } j = l = 1, 2, ..., N, & (5) \\ 0 \qquad \text{for other elements,} & \end{cases}$$

$$\mathbf{K}_{j,l} = \begin{cases} \dfrac{j^2+j-2}{2j+1} & \\ \qquad \text{for } j = l = 1, 2, ..., N, & \\ \displaystyle\int_{-1}^{\mu_a} P_j(\mu) P_{l-N-1}(\mu)\,\mathrm{d}\mu & \\ \qquad \text{for } j = 1, 2, ..., N \text{ and } l = N+1, ..., N+M, & \\ \displaystyle\int_{-1}^{\mu_a} P_{j-N-1}(\mu) P_l(\mu)\,\mathrm{d}\mu & \\ \qquad \text{for } j = N+1, ..., N+M \text{ and } l = 1, 2, ..., N, & \\ 0 \quad \text{for other elements.} & \end{cases} \qquad (6)$$

The viscosities μ_i and μ_e are that of the fluid inside and outside the bubble or drop, respectively, and both densities ρ_i and ρ_e are denoted similarly. Finally, the elements of the forcing vector **f** are

$$\mathbf{f}_j = \begin{cases} \dfrac{g\Delta\mathcal{V}}{4\pi R^3} & \text{for } j = 1, \\ 0 & \text{for } j = 2, 3, ..., N, \\ \displaystyle\int_{-1}^{\mu_a} \left(\frac{\Delta\eta(t,\mu)}{R} - \frac{\Delta\mathcal{V}(t)}{4\pi R^3} \right) P_{j-N}(\mu)\,\mathrm{d}\mu & \\ \qquad \text{for } j = N+1, ..., N+M. & \end{cases} \qquad (7)$$

In the forcing vector, g is the gravity acceleration. $\Delta\eta$ is the deformation of the interface in the parts, which are required to follow the motion of the capillary. ΔV is the imposed variation of the bubble or drop volume. The integration limit is $\mu_a = \cos\theta_a$.

By equation (2), the evolution of bubble shape is entirely described. It is possible to evaluate the response of the bubble or drop to volume variations or to motion of its support. The eigenmodes (their frequencies, damping rates and shapes) can be also obtained from (2) by standard methods.

2 Experiments

The oscillations of bubbles are studied experimentally by using a setup schematized in figure 2. In the setup, a bubble grows on a capillary. The bubble size is controlled by proper timing of valves, which either connect the capillary to a pressurized air, or drain it. The capillary can be moved by means of an electromagnetic coil, and a response of the bubble shape is recorded by a high-speed camera. By fitting the observed shapes of the bubble by (1), the values of b_j coefficients are experimentally determined. Several types of experiments can be performed, differing in the way how the capillary tip moves; experimental procedures are explained in detail in [9].

By moving the capillary tip periodically and by sweeping slowly across a frequency range, a frequency-response-function of the bubble to the motion of its support can be measured. Typical result (measured with $2R = 1$mm bubble, attached with attachment radius $2R_a = 0.32$ mm) is shown in figure 3. The amplitude of b_j coefficients (characterized by their root-mean-squares and normalized by the root-mean-square of the position

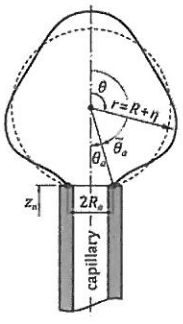

Fig. 1. Analyzed configuration.

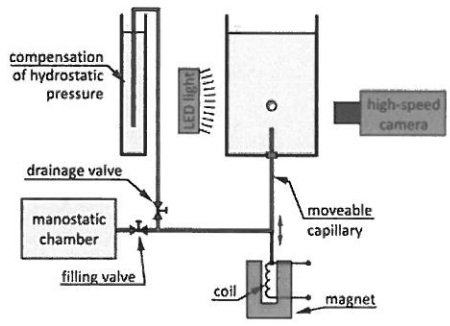

Fig. 2. Experimental setup.

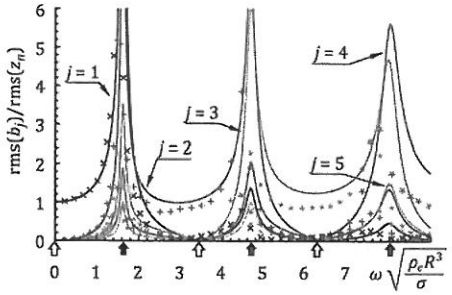

Fig. 3. Frequency response of a bubble to motion of its support.

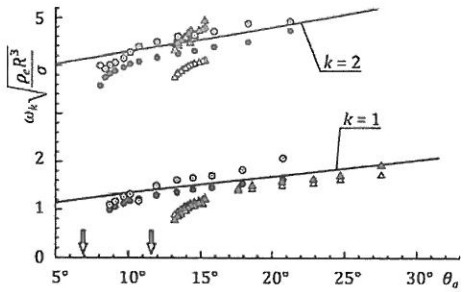

Fig. 4. Dependence of the eigenfrequency on attachment angle.

of the capillary tip) is plotted against the angular driving frequency ω (which is made dimensionless by normalizing by its scale $(\sigma/\rho_e R^3)^{1/2}$). Experimental measurements (points) and predicted frequency response (lines) are compared. Good agreement is found for the lower frequencies, while some disagreement is observed for higher frequencies. Still, the agreement is reasonable. Resonances are seen close to the predicted eigenfrequencies (black arrows). Close to the eigenfrequencies of a free (non-attached) bubble (white arrows), shape is described by a single b_j coefficient.

In a different kind of experiment, the capillary moves first with a frequency close to a resonant peak and this motion is then progressively stopped. The frequency and damping rate of the excited eigenmode can be determined from the consequent decaying oscillations [9]. Figure 4 shows the measured eigenfrequencies in dependence on the attachment angle θ_a (symbols without dots) and compares them with the predicted eigenfrequencies (lines). At higher attachment angles, the measured values follow correctly the predicted trend, but a larger deviation is observed for small θ_a. Noticeably, this deviation occurs when θ_a is close a value, at which detachment of the bubble occurs due to buoyancy; this value is around 7° and 11.6° for the data shown by circles and triangles, respectively, and these values are shown by arrows.

The deviation at small θ_a is linked with a formation of a neck, which forms as the bubble is about to detach due to buoyancy. The bubble shape, around which oscillations take place, becomes non-spherical, and this is not taken in account in the analytical solution. Unfortunately, the development of a theory for the non-spherical basic shape seems uneasy. To some extent, the decrease of the oscillation frequency can be estimated from the modification of the shape of bubble oscillations. As discussed in [9], it follows for the frequency of kth eigenmode from an energy balance,

$$\omega_k^2 = \frac{\dfrac{\sigma}{\rho_0 R^3}\cdot\sum_{j=1}^{N}\dfrac{j^2+j-2}{2j+1}\left(\dfrac{B_{kj}}{B_{kk}}\right)^2}{\sum_{j=1}^{N}\left(\dfrac{\rho_i}{\rho_0}\dfrac{1}{j(2j+1)}+\dfrac{\rho_e}{\rho_0}\dfrac{1}{(j+1)(2j+1)}\right)\left(\dfrac{B_{kj}}{B_{kk}}\right)^2}, \quad (8)$$

where $B_{kj} = \mathrm{rms}(b_j)$ for oscillations in the form of pure kth eigenmode. The eigenmode frequencies, determined from the observed shape of oscillations by means of the last equations, are also shown in figure 4 (symbols marked with an inside dot). Though the agreement is far from being perfect due to limited accuracy of experimental values of B_{kj}, the decrease of the frequency is still correctly reflected. This might have a practical implication to the characterization of interfacial properties, as the eigenmode frequency of the reference case with pure bubble or drop (with interface free of surfactants) could be estimated just from the observed oscillatory shape.

The effect of the neck formation on the eigenmode frequency can be characterized also empirically. In figure 5, a dimensionless frequency is shown in dependence on the ratio of the actual bubble volume to the volume, at which the detachment occurs. The eigenfrequency is normalized differently by taking the length scale λ_w in account, where

$$\lambda_w = \frac{4L}{2k+1} \quad (9)$$

is a characteristic wavelength of given eigenmode and it is determined by the arc length L of the meridian between the bubble apex and the attachment point, and k is the mode order [9]. As seen from figure 5, in this dimensionless expression, the eigenfrequencies of various modes more or less collapses to a master curve, which is, however, different for each mode order.

Figure 6 compares the measured damping rate of the lowest two eigenmodes (symbols without dots) with the predictions (lines). Similarly as in the case of frequency, the damping rate can be determined from the observed eigenmode shape [9]. It follows from the energy balance

$$\zeta_k = \frac{\dfrac{\mu_0}{\rho_0 R^2}\cdot\sum_{j=1}^{N}\left(\dfrac{\mu_i}{\mu_0}\dfrac{j-1}{j}+\dfrac{\mu_e}{\mu_0}\dfrac{j+2}{j+1}\right)\left(\dfrac{B_{kj}}{B_{kk}}\right)^2}{\sum_{j=1}^{N}\left(\dfrac{\rho_i}{\rho_0}\dfrac{1}{j(2j+1)}+\dfrac{\rho_e}{\rho_0}\dfrac{1}{(j+1)(2j+1)}\right)\left(\dfrac{B_{kj}}{B_{kk}}\right)^2}. \quad (9)$$

The damping rate determined using the last equation is shown in figure 6 by symbols denoted by dots. Again,

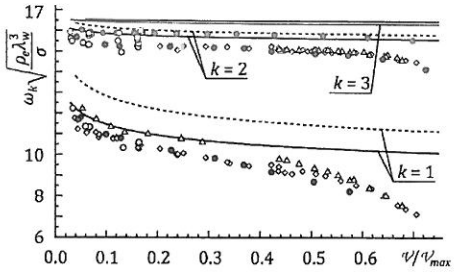

Fig. 5. Dependence of the eigenmode frequency on the volume-to-detachment-volume ratio

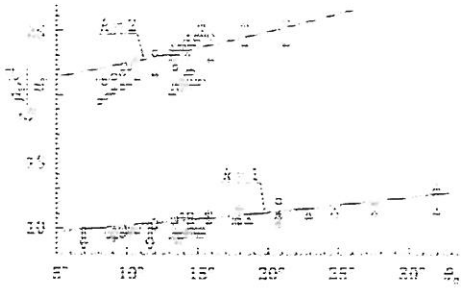

Fig. 6. Dependence of the eigenmode damping rate on the attachment angle.

similar trends between the measured values and those determined using (9) are observed. This again has a practical implication that the damping expected for a bubble or drop with pure interface (without surfactants) can be estimated from the observed shape of oscillations.

The damping rate can be also normalized with the use of λ_w as a characteristic length. In figure 7, such a dimensionless damping rate is plotted in dependence on the ratio of actual to the detachment bubble volume. It is observed that a constant value (different for each mode order) is found. The damping rate is hence determined uniquely by the characteristic wavelength λ_w on mode order k of the given eigenmode.

3 Conclusions

Results of analytical solution for bubble and drop oscillation have been presented. The analysis is able to predict a response of bubble or drop shape to variations of its volume and/or to motion of its support. The analytical results are compared to experiments, which were carried out for a bubble attached to a moveable capillary. Satisfactory agreement is found. The analysis, however, does not take in account a modification of the bubble shape due to buoyancy effects. For this reason, a deviation between the predicted and measured values increases as the bubble size approaches the size, at which a detachment due to buoyancy occurs. On the other hand, the oscillation frequency and the damping rate can be estimated from the observed shape of oscillations. This conclusion might have a practical implication for interpretation of experiments with bubbles or drops, which have surfactant molecules adsorbed at their interfaces.

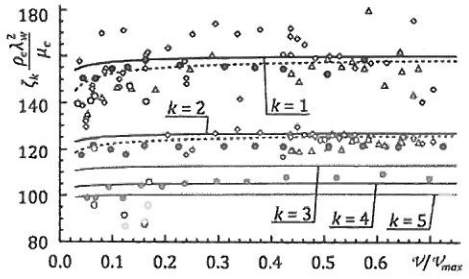

Fig. 7. Dependence of the eigenmode frequency on the volume-to-detachment-volume ratio

Acknowledgement

This research has been supported by Czech Science Foundation (project no. P101/11/0806).

References

1. T. J. Asaki, D. B. Thiessen, P. L. Marston, Phys. Rev. Letts. **75**, 2686 (1995)
2. N. Abi Chebel, J. Vejrazka, O. Masbernat, F. Risso, J. Fluid Mech. **702**, 533-542 (2012)
3. R. Miller, L. Liggieri, *Bubble and drop interfaces*, (Brill, Boston, Leiden 2011)
4. W. Meier, G. Greune, A. Meyboom, K. P. Hofmann, Eur. Biophys. J. Biophys. Letts. **29**, 113 (2000).
5. M. Strani, F. Sabetta, J. Fluid Mech. **141**, 233 (1984)
6. J. B. Bostwick, P. H. Steen, Phys. Fluids **21**, 032108 (2009)
7. A. Prosperetti, Phys. Fluids **24**, 032109 (2012)
8. S. Ramalingam, D. Ramkrishna, O. A. Basaran, Phys. Fluids **24**, 082102 (2012)
9. J. Vejrazka, L. Vobecka, S. Orvalho, M. Zednikova, J. Tihon, Phys. Fluids (submitted)

EFM12 Experimental Fluid Mechanics 2012
Hradec Králové 20th-23rd November 2012

Evaluation of material properties determining the moisture transfer

M. Vestfálova[1]

[1]KEZ, TU Liberec, Studentská 2, 461 17 Liberec 1, Czech Republic

Abstract. Due to solution the problems of moisture transfer is necessary to deal with two mechanisms of transfer: the molecular mass transfer and mass transfer by convection. Transfer driving force is the difference of concentrations of moisture, respectively the difference of partial vapour pressure. For molecular transfer is deciding value the coefficient of diffusivity, i.e. the property of the material. For mass transfer by convection is deciding the convection mass transfer coefficient, which depends on many parameters, but for one particular arrangement of the experiment will be influenced primarily velocity of the flow. Experimentally detectable is the overall moisture transfer caused by both mechanisms, i.e. the overall moisture transfer coefficient. Our goal was to attempt to evaluate the value of coefficient of diffusivity of some materials from the set of measured date. The date was obtained in different modes on different samples of materials. The next goal was to evaluate the dependence of the convection mass transfer coefficient on the speed of flow for the experiment alignment.

1 Introduction

The necessity to solute the problem of moisture transfer ensues on the Department of Power Engineering Equipment of Technical University of Liberec in connection on the solution of the project TA01020313. Its part was just the measurement of the amount of the transferred moisture of various materials. The experiment was executed by P. Dančová [1]. As the results of the measurement she obtained the mass flow of the vapour through various materials. For practise use of the results was necessary to evaluate "property" of the materials, best the coefficient of diffusivity.

2 Description of the experiment

In experimental measurements on the Department of Power Engineering Equipment of Technical University of Liberec [1] the moist air was flowing on both sides of the researched sample of material of rectangular shape. The airflow had the same temperature and pressure on either side of the sample. The air flow had lower relative humidity on the one hand of the material (we marked it "dry" air) and higher relative humidity beyond the material (we marked it "moist" air). The moister was transferred during the flow of air along the plate from the "moist" air to the "dry" air [2] and therefore the relative humidity of the air was changed on the both sides. The change of the relative humidity between input and output of both airflow was evaluated during the experiment. Experiment was conducted in two different modes of relative humidity of the "moist" air and in ten different modes of volume flow.

2.1 Measured values

During the experiment there was measured these values:

1. relative humidity of the „dry" air on the input (keeping in range 4.7 – 7.4%),
2. relative humidity of the „dry" air on the output,
3. relative humidity of the „moist" air on the input (first mode: 65 – 81%, second mode: 40 - 70%),
4. relative humidity of the „moist" air on the output,
5. temperatures of "dry" and "moist" air on the input and on the output (20 - 21 °C, isothermal process),
6. volume flow of the air through the exchanger (200 – 2000 l/hour., it is corresponding with speed of flow 0.26 – 2.6 m/s, ten modes),
7. pressure of "dry" and "moist" air on the input and on the output (barometric pressure just about 970 hPa).

2.2 Experimental samples

Ten different samples were measured:

1. sample S1: material "S", 2.6 g/m^2,
2. sample S2: material "S", 4.6 g/m^2,